Flow boiling of azeotropic and non-azeotropic mixtures. Effect of the glide temperature difference on the nucleate boiling contribution: assessment of methods

Flow boiling of azeotropic and non-azeotropic mixtures. Effect of the glide temperature difference on the nucleate boiling contribution: assessment of methods

R Mastrullo[1], A W Mauro[1], G Napoli[1], F Pelella[1], L Viscito[1]

[1] Department of Industrial Engineering, Federico II University of Naples, P.le Tecchio 80, 80125 Naples (Italy)
Corresponding author e-mail: wmauro@unina.it

Abstract. Due to the increasing concern about the global warming caused by the use of conventional refrigerants, new HFC/HFO blends are currently proposed to replace high-GWP substances. Most of them, however, present a considerable temperature glide that may negatively affect the nucleate boiling contribution to the heat transfer during evaporation. In this paper, flow boiling data of the new non-azeotropic mixtures R452A and R448A (carrying a high temperature glide of almost 5 °C) and of the conventional quasi-azeotropic blend R404A are provided in a horizontal stainless-steel tube having an internal diameter of 6.0 mm. For all the investigated fluids, the operating conditions explore mass fluxes from 150 to 600 kg/m^{2}s, saturation temperatures from 25 to 55 °C and imposed heat fluxes from 10 to 40 kW/m^2, in the whole range of vapor qualities. The nucleative boiling contribution is then isolated from the overall heat transfer coefficient data at disposal and the effect of the heat flux is discussed for both types of blends. Finally, the experimental values and trends are compared to different nucleate boiling correlations taken from literature and conceived for pure fluids, by testing some correction factors explicitly developed for high temperature glide substances.

1. Introduction

Conventional HFC refrigerants and their blends, currently used in the air-conditioning and refrigeration fields, are now facing a progressive phase-out due to the increasing concern about the global warming caused by these substances when released in the atmosphere. Depending on the application fields, the EU Regulation No 517/2014 [1] will limit the use of refrigerants with high GWP. Considering commercial refrigeration systems, as reviewed by Mota-Babiloni et al. [2], there is currently not a definitive solution to replace the mainly used refrigerant R404A. HFC/HFO (HydroFluoroOlephin) blends represent a possible solution: in particular, the 3-component non-azeotropic mixture R452A (R32/R125/R1234yf with a composition of 11%/59%/30% by weight) is designed with the aim to became a drop-in substitute of R404A without a complete re-design of principal cycle components [3]. R448A, instead, is a non-azeotropic mixture of R32 (26%), R125 (26%), R1234yf (20%), R134a (21%) and R1234ze(E) (7%). The overall system performance studies for the new R452A [3] [4] [5] [6] and R448A [7] [8] [9] [10] are limited. Furthermore, to the authors knowledge there are no experimental works related to the two-phase heat transfer for refrigerants R452A and R448A: experimental data for blends would be useful for an accurate design of evaporators and to give an assessment of the existing prediction methods. Moreover, the not negligible temperature glide during evaporation of these mixtures affects the nucleate boiling heat transfer contribution, with a higher required wall superheat to sustain the same bubble nucleation of a pure fluid in similar operating conditions [11].

The aim of this paper is therefore to present an experimental campaign on flow boiling heat transfer of refrigerants R452A and R448A in a single horizontal stainless-steel tube with an internal diameter of 6.0 mm. Tests have been performed by changing the refrigerants saturation (bubble) temperature from 25 to 55 °C, the mass flux from 150 to 600 kg/m^{2}s and the imposed heat flux from 10 to 40 kW/m^2, exploring all the vapor quality range up to x=1. The experimental results have been firstly compared to R404A data at the same operating conditions, by exploring the differences related to both convective and nucleative boiling contributions and quantifying the negative effect of the temperature glide on the nucleation phenomenon. The experimental data are then compared to some predictive methods for pure fluids and zeotropic mixtures, as well as a modified version of the Wojtan et al. [21] correlation.

2. Experimental facility

2.1. Refrigerant loop, water loop and test section

The schematic layout of the experimental apparatus and the tube test section is shown in Figure 1. The test rig is composed by a main refrigerant loop and a secondary loop for the control of the saturation temperature, which is set by a thermostatic bath. The main refrigerant loop, depicted by the black line in Figure 1 (a), is composed by a magnetic gear pump, a diabatic test section, a brazed plate condenser, a tube-in-tube sub-cooler, a liquid receiver and a micrometric throttling valve. A preheater is provided in order to control the vapor quality at the inlet of the tube test section. The secondary fluid in the condenser and subcooler heat exchangers is demineralized water, whose temperature is controlled by a thermostatic bath. Its circuit is displayed with a blue line in Figure 1(a). The test section employed is a smooth, horizontal, circular stainless-steel tube (type 316) with a measured internal diameter of 6.00±0.05 mm and an outer diameter of 8.00±0.05 mm. The measurement of the heat transfer coefficient takes place in point C shown in Figure 1(b), in which 4 thermocouples are fastened using a high-conductivity epoxy resin. More details on the test facility and on the measurement section are available in other previous publications [11], [12], [13], [14], [15].

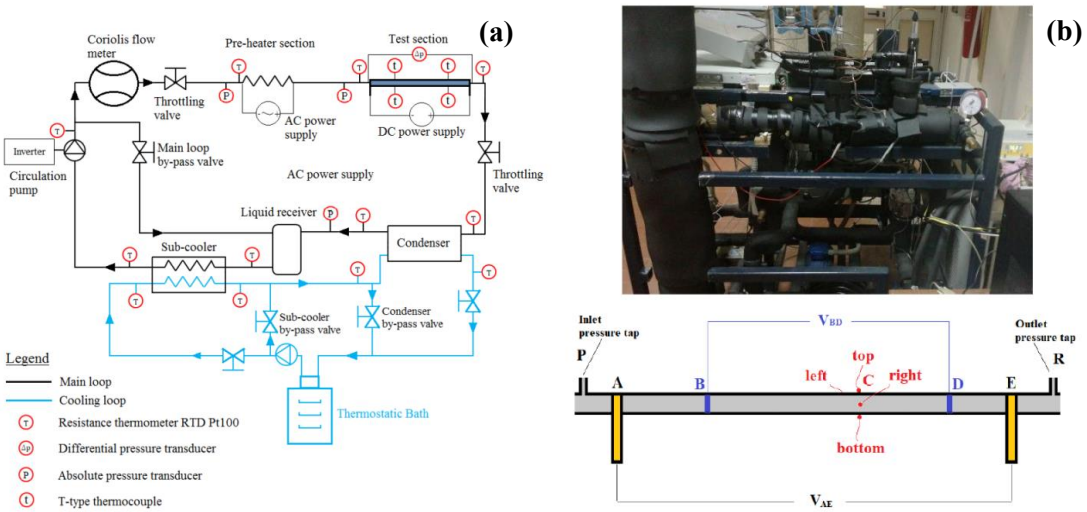

Figure 1. (a) Schematic lay-out of the flow boiling test rig; (b) Photograph and sketch of the test section.

2.2. Measurement instrumentation

Four T-type thermocouples are used to measure the wall temperatures for the evaluation of the heat transfer coefficients. These sensors are calibrated in-situ with two resistance thermometers having an overall estimated uncertainty of ±0.1 °C. The absolute pressure at the test section inlet is measured with an absolute pressure transducer having a measuring range of 0-35 bar and an overall uncertainty of ±0.5% of the read value. The pressure drop is instead estimated with a differential pressure transducer, whose total uncertainty is estimated to be ±0.06 kPa. The mass flow rate is measured by means of a

Coriolis flow meter, calibrated up to 2% of the full scale, with a maximum uncertainty of ±1% of the measurement. A digital wattmeter provides the heat applied to the preheater section, by separately measuring the voltage (100 mV-500 V) and current (1 mA-16 A). Its uncertainty is ±1.0% of the reading, as provided by the manufacturer. The heat flux applied to the test section requires the measurement of the DC voltage (electrical voltage transducer with an uncertainty of ±0.03% of the reading) and the DC current (directly measured by the DC power unit with an uncertainty of ±1.0%).

3. Method

3.1. Data reduction

The mean heat transfer coefficient can be evaluated using the Newton equation by assuming uniform heat flux q and an average wall temperature from the thermocouple positions (top, bottom, left and right side on the channel surface).

$$h_{mean} = \frac{q}{T_{wall} - T_{fluid}} = \frac{V_{BD} \cdot I_{tube}}{\pi d \overline{BD}} \cdot \frac{1}{T_{wall} - T_{fluid}} \tag{1}$$

$$T_{wall} = \frac{T_{wall,top} + T_{wall,bottom} + T_{wall,left} + T_{wall,right}}{4} \tag{2}$$

With the hypothesis of uniform heat generation in the metal tube and 1-D heat transfer in the radial direction, the inner wall tube temperature is evaluated by exploiting the thermocouple measuring at the outer tube surface:

$$T_{wall} = T_{th} + \frac{V_{BD} \cdot I_{tube}}{4\pi\lambda_{tube} \overline{BD}} \cdot \left[\left(D/d \right)^2 \cdot \left(1 - \ln\left(\left(D/d \right)^2 \right) \right) - 1 \right] \cdot \left[\left(D/d \right)^2 - 1 \right]^{-1} \tag{3}$$

The fluid saturation temperature T_{fluid} at the measurement point C (see Figure 1) is evaluated by using the measured inlet pressure, assuming a linear profile of the pressure drop along the diabatic test section. The local vapor quality calculation requires the evaluation of the local specific enthalpy, which is obtained with an energy balance on the heated section:

$$i_C = i_{in} + \frac{4 \cdot \overline{AC} \cdot q}{G \cdot d} \tag{4}$$

When considering R452A and R448A, the actual fluid temperature T_{fluid} as well as the local vapor quality is a function of both pressure and enthalpy due to their significant temperature glide. The test section inlet specific enthalpy, i_{in}, is instead computed with and energy balance applied on the preheater section, being dependent on the preheater load measured by the digital wattmeter and the preheater inlet enthalpy $i_{in,preh}$, (in sub-cooled liquid condition, obtained with measured temperature and pressure):

$$i_{in} = i_{in,preh} + \frac{\dot{Q}_{preh}}{\dot{m}} \tag{5}$$

3.2. Uncertainty analysis

The standard deviation in the recording time and the instrumental B-type uncertainties are considered for the measured parameters. The law of propagation of errors [16]-[17] is used for the uncertainty of the derived data. The maximum uncertainties are typically detected at the dry-out occurrence due to the higher fluctuations of the measured parameters. Most of the heat transfer coefficient results are collected within an overall uncertainty below ±13.0%. Exceptions are found at the occurrence of dry-out, due to the more significant fluctuations of the operating parameters in such conditions.

3.3. Experimental procedure and validation

Each test is performed and stored once the fixed mass flux, heat flux and system pressure reach steady state conditions. It is worth noting that, when using zeotropic mixtures, a constant system pressure is

not equivalent to a constant saturation temperature. Starting from low values of the vapor quality near to saturated liquid condition, approximately 10/15 data points are stored up to the dry-out occurrence and post-dry-out heat transfer. To ensure the steady state conditions during experiments, the uncertainty of operating parameters was calculated in real-time and the data acquisition could start only when the standard deviation of the working conditions during the recording time of 90 s was inferior to a chosen threshold (±0.2 °C for the wall temperatures, ±3% for the mass flux and ±0.10 °C for the liquid saturation temperature). The preheater and test section insulation as well as the correct functioning of the whole experimental apparatus have been previously verified with liquid single-phase experiments by using refrigerant R134a. Further detailed information on the validation procedure and results can be obtained from a previous work of the same authors with the same test facility [11].

4. Experimental results

4.1. Heat transfer coefficient results

For all the investigated fluids, the influence of the mass flux from 150 to 600 kg/m^{2}s, saturation temperature from 25 to 55 °C and imposed heat flux from 10 to 40 kW/m^2 on the heat transfer coefficient in the whole range of vapor qualities is investigated. Figure 2 (a) shows the trends of the average heat transfer coefficients as function of the vapor quality at high value of the mass flux (400 kg/m^{2}s) and low heat flux (10 kW/m^2).

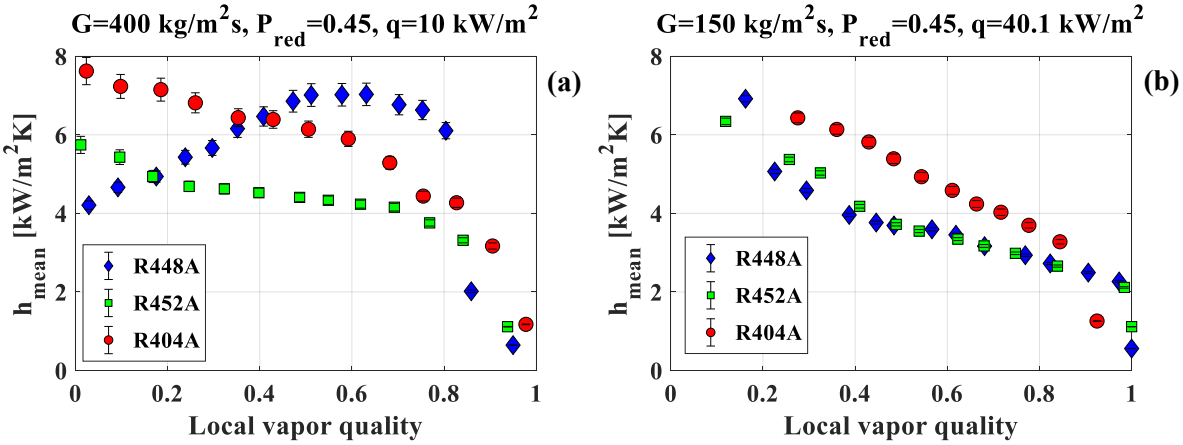

Figure 2. Effect of the investigated fluid on the mean heat transfer coefficient at T_{sat}=45.1°C for R404A, T_{sat}=43.9°C for R452A, T_{sat}=42.4°C for R448A: (a) G=400 kg/m^{2}s, q=10 kW/m^2, (b) G=150 kg/m^{2}s, q=40.1 kW/m^2.

Although these conditions promote the convective contribution to the heat transfer coefficient, only the experimental data of R448A assume a significant convective trend. The other fluids show instead a decreasing heat transfer coefficient as the vapor quality increases. Furthermore, there are not significant differences in terms of heat transfer coefficient between zeotropic and azeotropic mixtures.

The heat transfer coefficient behavior at conditions promoting the nucleative boiling contribution (low mass flux of 150 kg/m^{2}s and high imposed heat flux of 40 kW/m^2) is shown in Figure 2 (b). All fluids are characterized by a decreasing heat transfer coefficient with the vapor quality. It is important to note that heat transfer coefficient assumes lower value when considering zeotropic blends (R452A and R448A), suggesting a possible effect of the temperature glide on the nucleative boiling contribution.

4.2. Glide effect on boiling heat transfer

In order to clarify the effect of the temperature glide on the nucleative boiling contribution, in the following figures the heat transfer coefficient on the bottom side of the tube is considered. As can be seen in Figure 3(a)-(b), the bottom heat transfer coefficients are almost constant with vapor quality meaning that nucleate boiling is the only contribution to the heat transfer coefficient, especially for low-

medium value of the mass flux. On the contrary, the experimental data referred to the top heat transfer coefficient show a convective contribution not negligible or a decreasing trend with the vapor quality due to an anticipated dry-out, especially at low-medium mass flux.

In Figure 3(a) the bottom heat transfer coefficient at fixed mass flux and reduced pressure for the investigated azeotropic mixture (R404A) are shown, for two values of the heat flux. It is clear that passing from heat flux of 10 kW/m^2 to 40 kW/m^2, the heat transfer coefficients assume higher value with an increase up to +140%. Instead, when considering zeotropic blends, the bottom heat transfer coefficients show lower increments (+115%) with respect to the previous case, as show in Figure 3(b). This behavior then corroborates the hypothesis of a negative effect of the temperature glide on the nucleate boiling contribution.

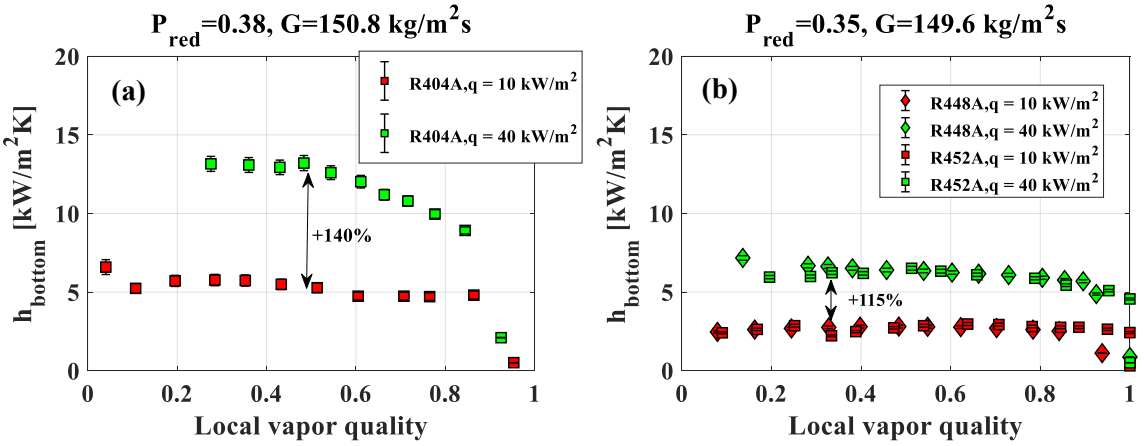

Figure 3. Effect of the heat flux on the bottom heat transfer coefficient: (a) azeotropic fluid R404A at G=150.8 kg/m^{2}s and T_{sat}=45.1°C; (b) zeotropic fluids R452A (T_{sat}=23.4°C) and R448A (T_{sat}=42.5°C) at G=149.6 kg/m^{2}s.

According to the asymptotic approach used in numerous prediction methods, the heat transfer coefficient can be expressed as a function of both nucleate and convective boiling contributions. In order to segregate the effect of the mass composition of the liquid on the nucleate boiling heat transfer coefficient, this last term has to be isolated. By using a reference state h_0, with the hypothesis of a constant convective contribution with varying heat flux, it is possible to fairly approximate (see the mathematical approach in [11]) the ratio of the nucleate boiling contribution to the ratio of the overall heat transfer coefficient as shown in equation (6) as far as the convective contribution h_{cb} is not predominant (h_{cb}<0.5h_0), as it happens for the bottom heat transfer coefficient data shown in Figure 3.

$$\frac{h_{NB}}{h_{NB,0}} \cong \frac{h}{h_0} \tag{6}$$

By considering the widely used correlation of Cooper [18], the boiling heat transfer coefficient ratio with respect to the reference state is a function of the heat flux ratio as shown in equation (7).

$$\frac{h_{NB}}{h_{NB,0}} = \left(\frac{q}{q_0}\right)^{0.67} \tag{7}$$

Several authors have proposed a modification of the typical boiling contribution by taking into account the resistance to mass diffusion in the liquid [19]. In the present paper the correction factor of Thome and Shakir [20] is considered giving a nucleative boiling heat transfer coefficient ratio as reported in equation (8).

$$\frac{h_{NB}}{h_{NB,0}} = \left(\frac{q}{q_0}\right)^{0.67} \cdot \left\{\left[1+\frac{h_{NB,0}\Delta T_{gl}}{q_0}\left(1-e^{-\frac{B}{\rho_L}\frac{q}{\Delta i_{LV}\rho_L}}\right)\right]\cdot\left[1+\frac{h_{NB}\Delta T_{gl}}{q}\left(1-e^{-\frac{B}{\rho_L}\frac{q}{\Delta i_{LV}\rho_L}}\right)\right]^{-1}\right\} \quad (8)$$

The effect of the heat flux on the experimental nucleate boiling heat transfer coefficients is shown in Figure 4(a) for R404A and Figure 4(b) for R452A and R448A. For each operating condition, a mean value of the bottom heat transfer coefficient is considered due to their not significant dependence on the vapor quality variation, and the reference value is 10 kW/m^2. When considering the azeotropic mixture R404A, the Cooper correlation (solid line), as well as the Thome and Shakir correction (dashed line), fit well the experimental data due to very low temperature glide, as shown in Figure 4(a). On the contrary, the Cooper correlation overrates the experimental data for zeotropic mixtures whereas they are fairly predicted with the Thome and Shakir correction for high-glide mixtures, as can be seen in Figure 4(b).

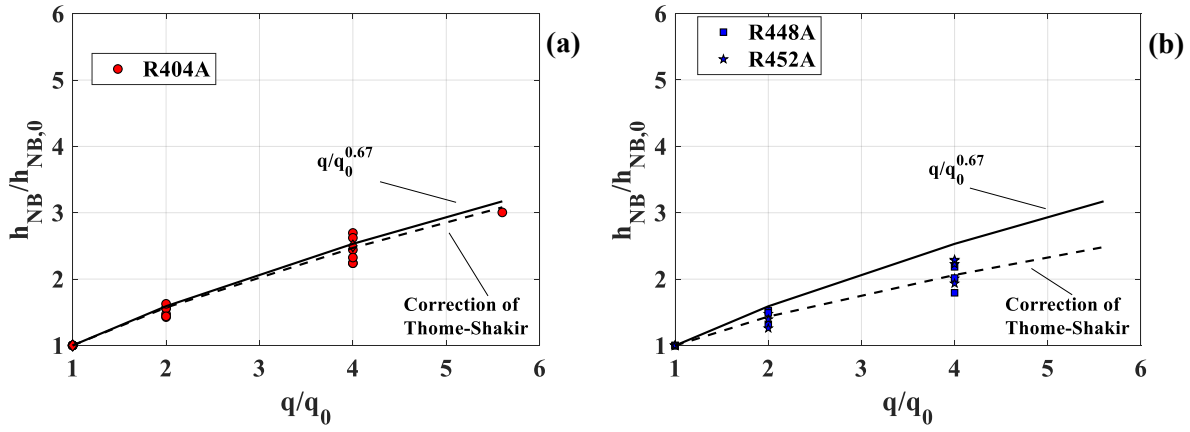

Figure 4. Effect of the heat flux variation on the bottom heat transfer coefficient and comparison with Cooper [18] and Thome and Shakir [20] correction for non-azeotropic mixtures: (a) R404A; (b) R452A and R448A.

5. Assessment of correlations

The average experimental heat transfer coefficients have been compared to some predictive methods, developed for both pure fluids and non-azeotropic blends. Figure 5(a)-(d) show the predicted heat transfer coefficient compared to the experimental data for some chosen models. Specifically, among the numerous correlations conceived for pure fluids or azeotropic mixtures, the flow pattern based method of Wojtan et al. [21] and the well-known superposition model of Gungor and Winterton [22] are here employed. The first provides a calculated *MAE* of 45.8% for the entire database, whereas the correlation of Gungor and Winterton gives a *MAE* of 32.8%, with 52.8% of the points falling in a ±30% error band. As reviewed by [23], several correlations have also been developed for zeotropic mixtures. Among them, the correlation of Mirsha et al. [25] was developed on the experimental results of R12/R22 mixtures in annular flow and works well with our experimental data (*MAE* of 24.5%). The method proposed by Guo et al. [26] was obtained by modifying the model presented by Liu and Winterton [27] based on their experimental results for a R134a/R245fa mixture, but largely overestimates the heat transfer coefficients (*MAE* of 64.8%). Bivens and Yokozeki [28] also proposed a modification of the Jung et al. [29] and Wattelet et al. [30] correlations, also overpredicting the present database for both R404A and zeotropic mixtures (*MAE* of 44.1%). Finally, the model developed by Mastrullo et al. [11] for their R452A data is also used for the present assessment. This correlation modifies the Wojtan et al. flow pattern based method by multiplying the nucleative boiling contribution to the correction factor of Thome and Shakir, as shown in the previous analysis. The agreement with the present database is satisfactory and improved with respect of the original Wojtan et al. correlation, having *MAE* of 36.2%, 36.6% and 33.8% when used respectively with R404A, R448A and R452A.

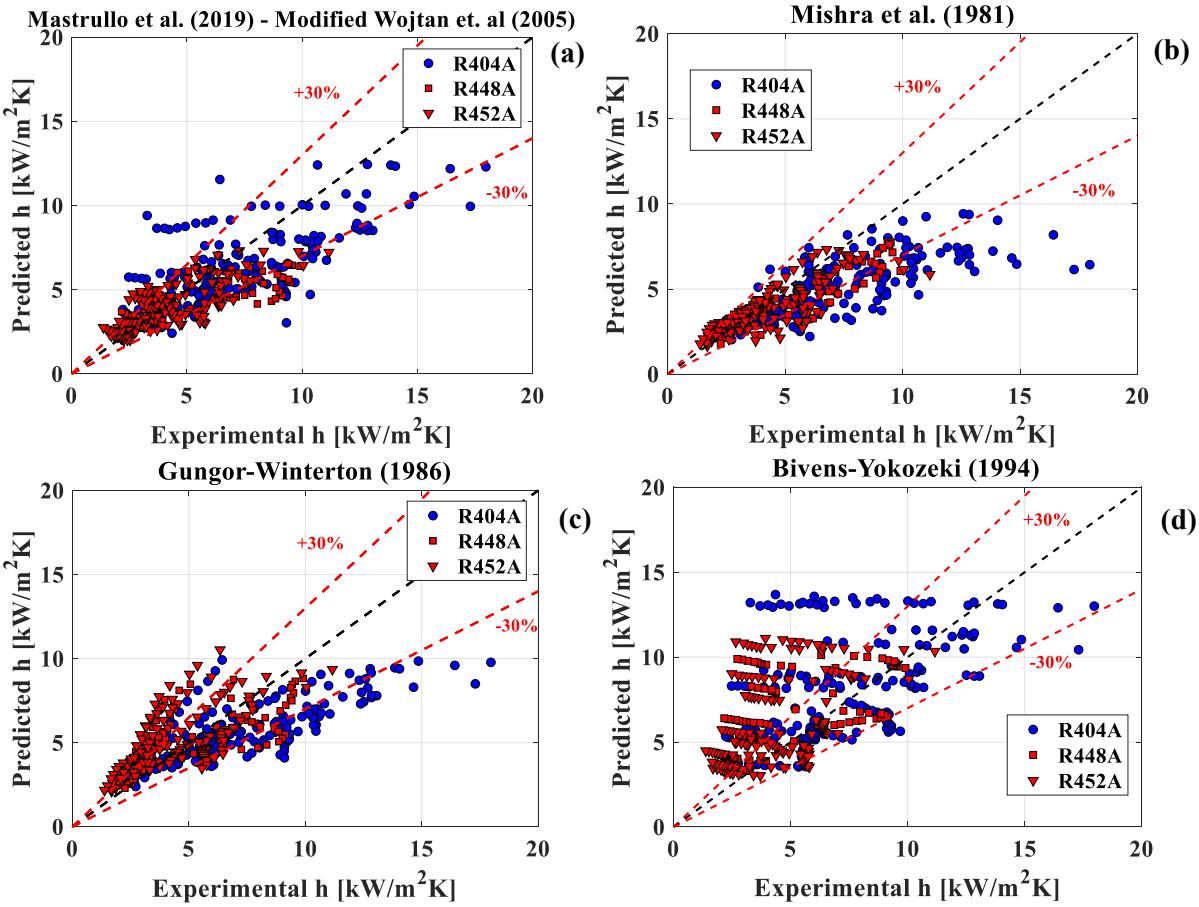

Figure 5. Experimental versus predicted average two-phase heat transfer coefficients. (a) Mastrullo et al. (2019) (Modified Wojtan et al. (2005)) [11]. (b) Mishra et al. (1981) [25]. (c) Gungor and Winterton (1986). (d) Bivens-Yokozeki (1994) [28].

6. Conclusions

An experimental analysis on the two-phase boiling heat transfer of zeotropic (R452A and R448A) and azeotropic blend R404A has been carried-out in a single horizontal circular tube with an internal diameter of 6.0 mm. A detailed analysis to quantify the effect of the temperature glide on the nucleate boiling heat transfer is also shown. The main conclusions are listed below:

- The effect of the temperature glide on the mean heat transfer coefficient seems more evident in conditions promoting the boiling contribution (low-medium mass flux and high heat flux).
- The positive influence of the heat flux on the heat transfer coefficient is lower when considering zeotropic mixtures due to their high temperature glide. The Thome and Shakir [20] correction successfully quantifies this effect based on the present experimental database.
- The assessment of different two-phase heat transfer predictive methods for pure fluids and zeotropic mixtures has shown that the correlation of Mirsha et. al [25], developed for zeotropic mixtures, predicts the experimental data with a *MAE* of 24.5%.

Acknowledgments

Luca Viscito received a grant at Federico II University of Naples (Italy), Department of Industrial Engineering. Funded by Ministero dell'Istruzione dell'Università e della Ricerca (MIUR), via the project PRIN2015 “Clean Heating and Cooling Technologies For An Energy Efficient Smart Grid”, which is gratefully acknowledged.

References

[1] European Parliament and the Council of the European Union. Directive 2006/40EC of the European Parliament and of the Council of 17 May 2006 relating to emissions from air conditioning systems in motor vehicles and amending Council Directive 70/156/EC, Off J Eurp Union, col. 161; 2006, 1-11
[2] Mota-Babiloni A, Navarro-Esbri J, Barragan-Cervera A, Molés F, Peris B and Verdu G 2015 *Int. J. Refr.* **57** 186-196
[3] Marek Z and Sedliak J 2015 F-Gases EU Regulation: R404A Replacement Refrigerants – Compressor Manufacturer Experience
[4] Mota-Babiloni A, Makhnatch P and Khodabandeh R 2017 *Int. J. Refr* **82** 288-301
[5] Li G 2017 *Sust. En. Techn. Assessm.* **21** 33-49.
[6] American Society of Heating, Refrigerating and Air-Conditioning Engineers, Inc. ASHRAE Standard 34 Designation and Safety Classification of Refrigerants; 2013.
[7] Wang B, Cheng Z, Shi W and Li X 2018 *Int. J. Refr.* **98** 343-353
[8] Yana Motta S F, Becerra E W and Spatz M W 2012 *International refrigeration and air conditioning conference*. Paper 1351
[9] Sethi A, Pottker G and Yana Motta S 2016 *Science and Technology for the Built Environment* **22** 1175-1184.
[10] Beshr M, Aute V, Sharma V, Abdelaziz O, Fricke B and Radermacher R 2015 *Int. J. Refr.* **56** 154-164.
[11] Mastrullo R, Mauro A W and Viscito L 2019 *Exp. Therm. Fl. Sc*. **105** 247-260
[12] Lillo G, Mastrullo R, Mauro A W and Viscito L 2019 *Int. J. Heat Mass Transf.* **129** 547-561
[13] Lillo G, Mastrullo R, Mauro A W and Viscito L 2019 *Int. J. Refr.* **97** 143-156
[14] Mastrullo R, Mauro A W, Revellin R and Viscito L 2018 *Appl. Therm. Eng.* **145** 251-263
[15] Lillo G, Mastrullo R, Mauro A W and Viscito L 2018 *Int. J. Heat Mass Transf.* **126** 1236-1252
[16] Moffat R J 1982 *Trans. ASME: J. Fl. Eng.* **104** 250-260
[17] Moffat R J 1985 *Trans. ASME: J. Fl. Eng.* **107** 173-178
[18] Cooper M 1984 *Adv. Heat Transf.* **16** 157–239
[19] Grauso S, Mastrullo R, Mauro A W and Vanoli G P 2011 *Int. J. Refr* **34** 1028–1039
[20] Thome J R and Shakir S 1987 *AIChE Symp. Ser.* **83** 46–51
[21] Wojtan L, Ursenbacher T and Thome J R 2005 *Int. J. Heat Mass Transf.* **48** 2970–2985.
[22] Gungor K and Winterton R 1986 *Int. J. Heat Mass Transf.* **29** 351–358
[23] Zhang J, Mondejar M E and Haglind F 2019 *Appl. Therm. Eng.* **150** 824-839
[24] Kim S M and Mudawar I 2013 *Int. J. Heat Mass Transf.* **64** 1226–1238
[25] Mishra M P, Varma H K and Sharma C P 1981 *Lett. Heat Mass Transf.* **8** 127–136
[26] Guo C, Wang J, Du X and Yang L 2016 *Appl. Therm. Eng.* **103** 901–908
[27] Liu Z and Winterton R H S 1991 *Int. J. Heat Mass Transf.* **34** 2759–2766
[28] Bivens D B and Yokozeki A 1994 *Proc. Int. Ref. Air Cond. Conf. (Purdue)* 299–304.
[29] Jung D S, McLinden M, Radermacher R and Didion D 1989 *Int. J. Heat Mass Transf.* **32** 1751–1764.
[30] Wattelet J P, Chato J C, Souza A L and Christofferson B R 1993 *ACRC TR-41* (Urbana, Illinois)